Hindawi Publishing Corporation
Journal of Chemistry
Volume 2013, Article ID 627582, 6 pages
http://dx.doi.org/10.1155/2013/627582

Research Article

Investigation on the Structure and Electrochemical Properties of La-Ce-Mg-Al-Ni Hydrogen Storage Alloy

Yuqing Qiao,[1,2] Jianyi Xi,[2] Minshou Zhao,[2] Guangjie Shao,[2] Yongchun Luo,[3] and Limin Wang[1]

[1] *State Key Laboratory of Rare Earth Resources Utilization, Changchun Institute of Applied Chemistry, CAS, Changchun 130022, China*
[2] *College of Environmental and Chemical Engineering, Yanshan University, Qinhuangdao, Hebei 066004, China*
[3] *Department of Materials Science and Engineering, Lanzhou University of Technology, Lanzhou, Gansu 730050, China*

Correspondence should be addressed to Yuqing Qiao; qiaoyq@ysu.edu.cn and Limin Wang; lmwang@ciac.jl.cn

Received 28 October 2013; Accepted 23 November 2013

Academic Editor: Xinqing Chen

Structure and electrochemical characteristics of $La_{0.96}Ce_{0.04}Mg_{0.15}Al_{0.05}Ni_{2.8}$ hydrogen storage alloy have been investigated. X-ray diffraction analyses reveal that the $La_{0.96}Ce_{0.04}Mg_{0.15}Al_{0.05}Ni_{2.8}$ hydrogen storage alloy consisted of a (La, Mg)Ni_3 phase with the rhombohedral $PuNi_3$-type structure and a $LaNi_5$ phase with the hexagonal $CaCu_5$-type structure. TEM shows that the alloy is multicrystal with a lattice space 0.187 nm. EDS analyse shows that the content of Mg is 3.48% (atom) which coincide well with the designed composition of the electrode alloy. Electrochemical investigations show that the maximum discharge capacity of the alloy electrode is 325 mAh g^{-1}. The alloy electrode has higher discharge capacity within the discharge current density span from 60 mA g^{-1} to 300 mA g^{-1}. Electrochemical impedance spectroscopy measurements indicate that the charge transfer resistance R_T on the alloy electrode surface and the calculated exchange current density I_0 are 0.135 Ω and 1298 mA g^{-1}, respectively; the better eletrochemical reaction kinetic of the alloy electrode may be responsible for the better high-rate dischargeability.

1. Introduction

La-Mg-Ni system alloys are promising materials owing to their higher electrochemical capacity compared to AB_5-type alloys; however, the poor cycling stability and HRD of the La-Mg-Ni hydrogen storage alloys have prevented it from being practically used as electrode alloys for Ni-MH battery [1–14]. According to the literature [15], the capacity degradation during cycling of La-Mg-Ni based hydrogen storage electrode alloy is influenced mainly by two factors: the passivation due to the formation of $La(OH)_3$ and $Mg(OH)_2$ on the alloy surface and the accelerated corrosion rate of the active components due to the large molar volume of hydrogen V_H of the alloy hydrides. As the alloy electrode with a large V_H undergoes a large cell volume expansion/contraction during charge/discharge cycle, a higher degree of pulverization resulted and thus more surface area is exposed to the corrosive electrolyte, which would lead to a lower cycling stability [16–18].

The partial substitution of Al for Ni in La-Mg-Ni based alloy can improve the cycling stability due to the noticeable decrease in the cell volume expansion rate ($\Delta V/V$) on hydriding [19, 20]. According to the literature [21], Al was helpful to the formation of $LaNi_5$ phase in $La_{0.67}Mg_{0.33}Ni_{3.0-x}Al_x$ ($x = 0, 0.1, 0.2, 0.3$) hydrogen storage alloys. $LaNi_5$ phase with $CaCu_5$ type appeared when Al was added. The increase of Al content leads to an increase of content of $LaNi_5$ phase, and the main phase of the alloy is $LaNi_5$ phase with $x = 0.3$. According to the literature [22, 23], rare earth elements (such as Dy and Pr) are helpful to decrease the cell volume of $LaNi_5$ phase. For V-based solid solution alloy [24], the addition of Ce can improve the dynamic performance, which makes the charge transfer resistance (R_T) decrease and the exchange current density (I_0) increase markedly. Just for

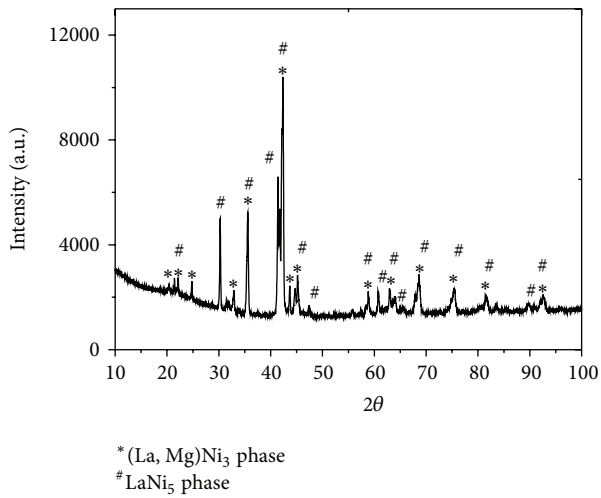

FIGURE 1: X-ray diffraction patterns of $La_{0.96}Ce_{0.04}Mg_{0.15}Al_{0.05}Ni_{2.8}$ alloy.

those considerations, Al has been used to partly substitution for Ni, Ce has been used to partly substitution for La, and the structure and electrochemical properties of the La-Ce-Mg-Al-Ni hydrogen storage electrode alloy have been investigated in this paper.

2. Experimental

$La_{0.96}Ce_{0.04}Mg_{0.15}Al_{0.05}Ni_{2.8}$ hydrogen storage electrode alloy was prepared by induction melting under argon and then remelted to ensure for homogeneity. The purity of the individual starting metal was higher than 99.5 mass%. The prepared electrode alloy was mechanically crushed to particles and then pulverized to a fine powder of about 300 mesh, and the sample powder was used for XRD, TEM, and electrochemical characteristics. Crystal structure of La-Ce-Mg-Al-Ni hydrogen storage electrode alloy was investigated by XRD (CuKα, Si internal standard) on Rigaku D/max 2500pc X-ray diffraction meter using JAD5 software and by TEM on JEM-2010.

The metal hydride electrode was prepared by pressing the mixture of alloy powder with carbonyl nickel powder in a weight ratio of 1 : 5 into a tablet with a diameter about 10 mm and a thickness about 1.5 mm. The electrochemical properties were performed on a DC-5 battery testing instrument using a half-cell system which consists of a metal hydride electrode as the negative electrode and a sintered $Ni(OH)_2$/NiOOH electrode with excess capacity in 6 mol L^{-1} KOH electrolyte solution; the cut-off voltage for discharge was 0.8 V.

Electrochemical impedance spectroscopy (EIS) was used to clarify the kinetic properties of dehydrating action, such as the charge-transfer resistance (R_T) and the exchange current density (I_0). After the test electrodes were completely activated, EIS measurements were conducted at 50% depth of discharge (DOD) using a Solartron SI1187 electrochemical interface with ZPLOT electrochemical impedance software and 1255B frequency response analyzer. The EIS spectra of the electrodes were obtained in the frequency range from 100 kHz to 10^{-2} Hz with alternating current amplitude of 5 mV under open-circuit conditions. According to the analysis model proposed by Kuriyama et al. [26], an equivalent circuit for the alloy electrode was used and the parameters in the equivalent circuit were fitted using least-square method with ZVIEW electrochemical impedance software; I_0 is calculated from the following formulation ($I_0 = RT/FR_T$).

3. Result and Discussion

3.1. XRD. Figure 1 shows the XRD patterns of $La_{0.96}Ce_{0.04}Mg_{0.15}Al_{0.05}Ni_{2.8}$ alloy. It can be seen that the alloy consists of a (La, Mg)Ni_3 phase with the rhombohedral $PuNi_3$-type structure (space group: $R\bar{3}$ m (166)) and a $LaNi_5$ phase with the hexagonal $CaCu_5$-type structure (space group: P6/m^3 (191)). This result coincides well with that reported by Zhang et al. [21] and Liao et al. [15]: Al was helpful to the formation of $LaNi_5$ phase with $CaCu_5$ type in La-Mg-Ni hydrogen storage alloys, and also the content of Al decides the content of $LaNi_5$ phase. According to the literature, about 2% Al has been used to substitute for Ni in the La-Mg-Ni alloy in this paper to form $PuNi_3$-type structure and $CaCu_5$-type structure.

The lattice parameters of a, c, and the cell volume of $LaNi_5$ phase are 0.5012 nm, 0.3984 nm, and 86.7×10^{-3} nm^3, respectively. Each one of those parameters is smaller than the relevant one of La-Mg-Al-Ni alloy [25] (a = 0.5058 nm, b = 0.4042 nm, cell volume = 89.5×10^{-3} nm^3), respectively. According to the literature [22, 23], rare earth elements (such as Dy and Pr) were helpful to decrease the cell volume of $LaNi_5$ phase, as shown in Table 1. The cell volume of $LaNi_5$ phase without rare earth element was larger than 87×10^{-3} nm^3, while it is smaller than 87×10^{-3} nm^3 for the alloys with rare earth element. It should be pointed out that the smaller the cell volume of the main phase ($LaNi_5$ phase) would decrease the cell volume expansion rate ($\Delta V/V$) on hydriding, and it is favorable for the alloy to decrease pulverization.

3.2. TEM. Figure 2 shows the TEM and EDS micrographs of $La_{0.96}Ce_{0.04}Mg_{0.15}Al_{0.05}Ni_{2.8}$ electrode alloy. It is obvious that the alloy is composed of multicrystal. The lattice space d can be calculated from the following formulation ($d = \lambda L/r$), where L means the length of the camera (0.2 m), λ means the wavelength of the accelerated voltage (0.00370 nm), and r means the radius of the diffractive spot (0.593 cm). The result shows that the d is 0.187 nm.

The phase composition of the alloy has been semiquantitatively analyzed with EDS which is shown in Figure 2 and the results are shown in Table 2. It can be seen that electrode alloy is composed of La, Ce, Mg, Al, and Ni, and the content of Mg is 3.48% (atom), which coincide well with the designed composition of the electrode alloy.

3.3. Cycle Stability and Discharge Profile. The cycle stability of $La_{0.96}Ce_{0.04}Mg_{0.15}Al_{0.05}Ni_{2.8}$ alloy electrode is shown in Figure 3(a). The alloy electrode is gradually activated during

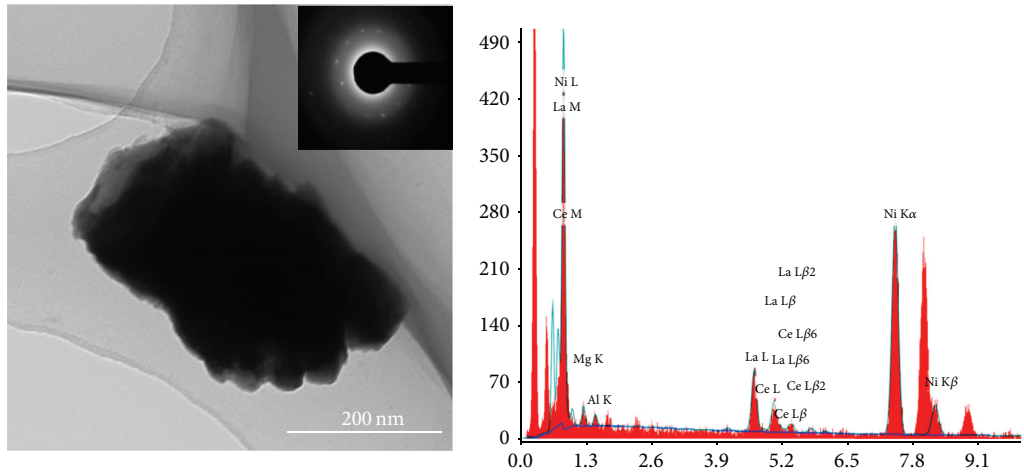

Figure 2: TEM and EDS $La_{0.96}Ce_{0.04}Mg_{0.15}Al_{0.05}Ni_{2.8}$ alloy.

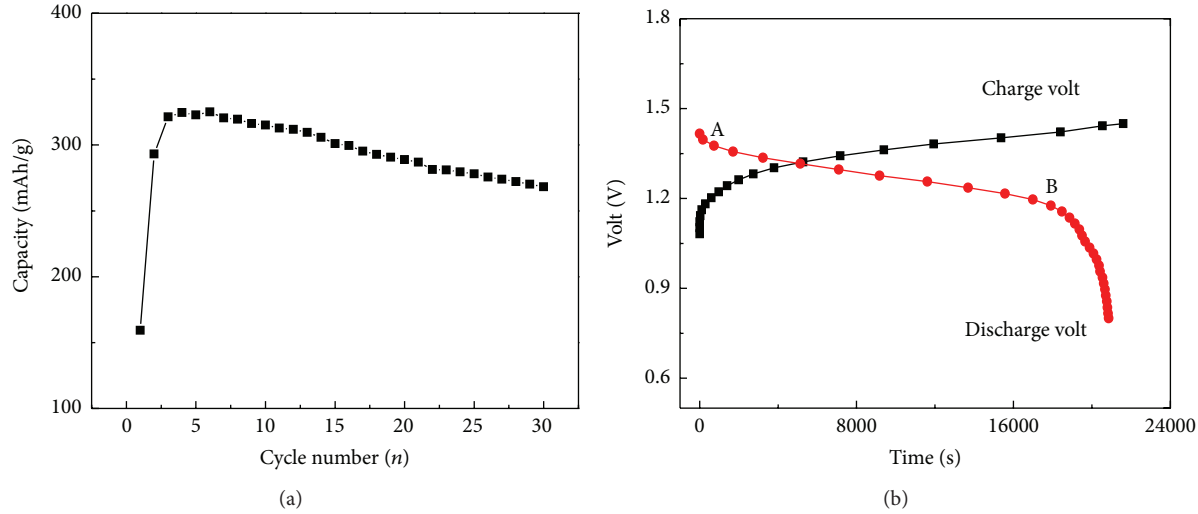

Figure 3: Discharge capacity and discharge profile for $La_{0.96}Ce_{0.04}Mg_{0.15}Al_{0.05}Ni_{2.8}$ alloy.

charge/discharge cycle process and reached maximum discharge capacity of 325 mAh g^{-1} at 4th cycles to be proved to have the higher electrochemical activity. According to the literature [21], Al was helpful to the formation of $LaNi_5$ phase in La-Mg-Ni hydrogen storage alloys, but the content of Al would lead to some decrease in discharge capacity. The result also shows that the discharge capacity at 30th cycles is 268 mAh g^{-1}, which is about 82.5% of the maximum discharge capacity (325 mAh g^{-1}), and implies that cycle stability of the alloy electrode is acceptable.

Figure 3(b) shows the typical discharge capacity-potential curves for $La_{0.96}Ce_{0.04}Mg_{0.15}Al_{0.05}Ni_{2.8}$ alloy electrode. It can be clearly seen that the alloy electrode has a wider discharge voltage plateau. It is about 4.5 h for the battery to hold the discharge voltage above 1.2 V with a wider discharge voltage plateau from 1.38 V to 1.20. It was reported by Iwakura et al. [27] that the curve of equilibrium potential-discharge capacity and the curve of P-C isotherm were rather coordinate, especially for the tendency of the plateau region; that was to say, the plateau region of equilibrium potential for $La_{0.96}Ce_{0.04}Mg_{0.15}Al_{0.05}Ni_{2.8}$ alloy electrode has a good discharge characteristics.

3.4. Temperature Effect and High-Rate Dischargeability. Figure 4(a) shows the dependence of the discharge capacity of $La_{0.96}Ce_{0.04}Mg_{0.15}Al_{0.05}Ni_{2.8}$ alloy electrode on different temperatures. As can be seen in the figure, the discharge capacity of the alloy electrode is decreased as the temperature increased from 303 K to 333 K. For example, the discharge capacity of the alloy electrode is 284 mAh g^{-1} and 263 mAh g^{-1} at 323 K and at 333 K, respectively. It implies that the discharge capacity of $La_{0.96}Ce_{0.04}Mg_{0.15}Al_{0.05}Ni_{2.8}$ alloy electrode is sensitive to temperature within the temperature span.

HRD is an important property of electrode alloy used as negative electrode material in Ni-MH battery, especially

Table 1: Lattice constant and cell volume for La-RE-Mg-Al-Ni phydrogen storage alloys [22, 23, 25].

Alloy	a/nm	c/nm	$V\times 10^{-3}$/nm^3
La-Mg-Al-Ni	0.5058	0.4042	89.5
La-Ce-Mg-Al-Ni	0.5012	0.3984	86.7
$(La_{1-x}\ Dy_x)_{0.8}Mg_{0.2}Ni_{3.4}\ Al_{0.1}$ ($x = 0$)	0.5024	0.3982	87.0
$(La_{1-x}\ Dy_x)_{0.8}Mg_{0.2}Ni_{3.4}\ Al_{0.1}$ ($x = 0.05$)	0.5019	0.3978	86.8
$(La_{1-x}\ Dy_x)_{0.8}Mg_{0.2}Ni_{3.4}\ Al_{0.1}$ ($x = 0.2$)	0.4993	0.3909	84.4
$La_{0.8-x}\ Pr_xMg_{0.2}Ni_{3.8}$ ($x = 0$)	0.5028	0.3989	87.3
$La_{0.8-x}\ Pr_xMg_{0.2}Ni_{3.8}$ ($x = 0.15$)	0.5012	0.3983	86.7
$La_{0.8-x}\ Pr_xMg_{0.2}Ni_{3.8}$ ($x = 0.40$)	0.4998	0.3982	86.1

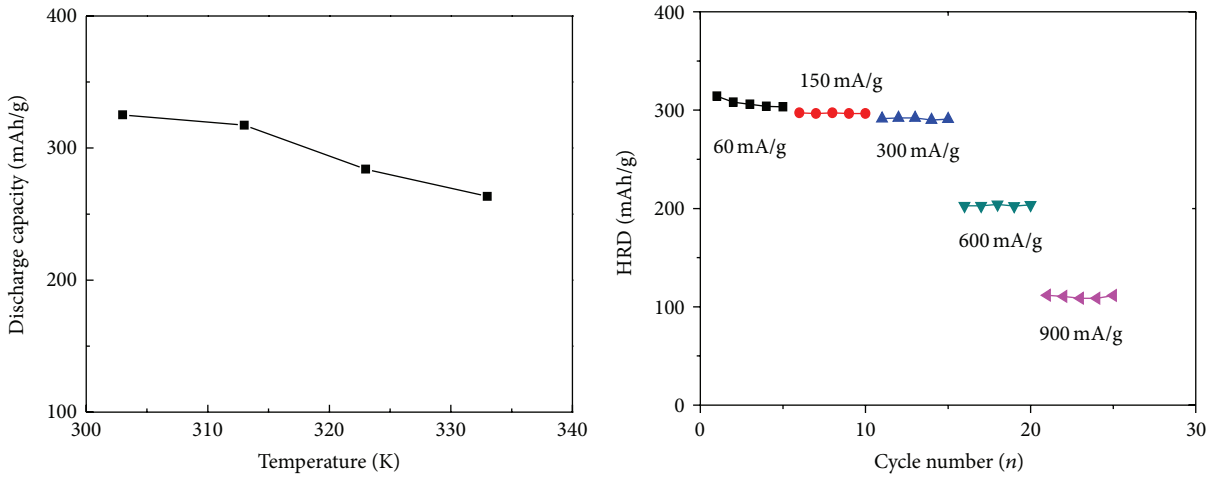

Figure 4: Effect of temperature and discharge current density on the discharge capacity for $La_{0.96}Ce_{0.04}Mg_{0.15}Al_{0.05}Ni_{2.8}$ alloy.

Table 2: Phase composition and interplanar distance for $La_{0.24}Ce_{0.01}Mg_{0.04}Al_{0.01}Ni_{0.70}$ alloy.

Composition (atom %)					d (nm)
La	Ce	Mg	Al	Ni	
23.93	1.29	3.48	1.47	69.82	0.187

used in electric vehicles. Figure 4(b) shows the relationship between the discharge capacity and the discharge current density of $La_{0.96}Ce_{0.04}Mg_{0.15}Al_{0.05}Ni_{2.8}$ alloy electrode. It can be clearly seen that the alloy electrode has higher discharge capacity within the discharge current density span from 60 mA g^{-1} to 300 mA g^{-1}, and the cycle stability of alloy electrode is accepted. It is worthy of notice that the discharge capacity of the alloy electrode is higher than 200 mAh g^{-1} at 600 mA g^{-1} and 100 mAh g^{-1} at 900 mA g^{-1}, respectively. This characteristic of the alloy is crucial for it to be used as a negative electrode material of Ni-MH batteries.

3.5. EIS. Figure 5 shows the EIS of $La_{0.96}Ce_{0.04}Mg_{0.15}Al_{0.05}Ni_{2.8}$ alloy electrode at 50% DOD. EIS has been used for determining R_T and I_0 to clarify the kinetic properties of dehydrating action at 303 K. According to the equivalent circuits [26], the large semicircle in the low-frequency region

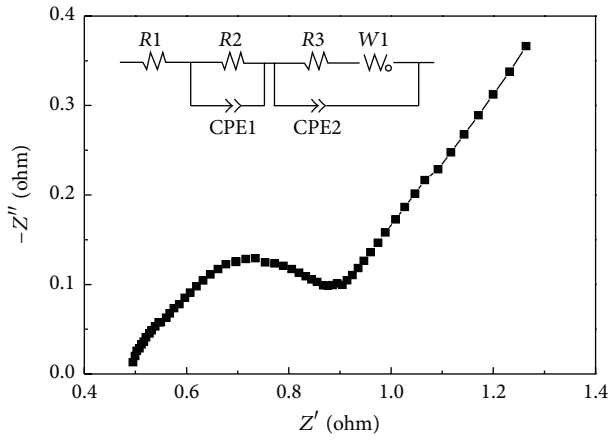

Figure 5: EIS of $La_{0.96}Ce_{0.04}Mg_{0.15}Al_{0.05}Ni_{2.8}$ alloy electrode at 50% DOD.

is attributed to the charge transfer resistance R_T on the alloy surface, and the fitted result shows that the R_T is 0.135 Ω. The exchange current density I_0 for the alloy electrode can be calculated by the following formulation: $I_0 = RT/FR_T$, where R, T, F, and R_T denote the gas constant, the absolute temperature, the Faraday constant, and charge transfer resistance on

Table 3: Self-discharge characteristics of $La_{0.96}Ce_{0.04}Mg_{0.15}Al_{0.05}Ni_{2.8}$ alloy electrode at 293 K.

Day	C_1/mAh^{-1}	C_2/mAhg^{-1}	C_3/mAhg^{-1}	C_1–C_3/mAhg^{-1}	C_3-C_2/mAhg^{-1}	Self-discharge rate/%
1	296.1	283.3	293.2	2.9	9.9	3.9
2	287.5	270.8	383.1	4.4	12.3	5.1
4	278.9	190.3	258.2	20.7	67.9	7.3

the alloy surface, respectively. The calculated result shows that I_0 is 1298 mA g^{-1}, which is much larger than that in V-based solid solution electrode alloy [28]. This may be responsible for the better high-rate dischargeability.

3.6. Self-Discharge. According to the literature [29], self-discharge of the hydrogen storage alloy can be divided into two parts, the reversible (C_3-C_2) and irreversible (C_1–C_3), respectively. The self-discharge rate of the alloy electrode can be calculated with $\{1 - 2C_2/(C_1 + C_3)\} \times 100\%$ day. C_1, C_2, and C_3 have been determined with the tested alloy electrode standing at open circuit for 1, 2, and 4 days, respectively, as shown in Table 3. The results indicate that the self-discharge rate of the alloy electrode is increased as the time standing increased from 1 day to 4 days, also, the reversible part (C_3-C_2) which due to desorption of hydrogen is larger than that of irreversible (C_1–C_3) part which was due to deterioration of the hydrogen storage alloy.

4. Conclusion

The structure and electrochemical properties of $La_{0.96}Ce_{0.04}Mg_{0.15}Al_{0.05}Ni_{2.8}$ alloy electrode have been studied. The conclusions can be drawn as follows.

(1) The hydrogen storage alloy is consisted of a (La, Mg)Ni_3 phase with the rhombohedral $PuNi_3$-type structure and a $LaNi_5$ phase with the hexagonal $CaCu_5$-type structure.

(2) The maximum discharge capacity 325 mAh g^{-1} and cyclic stability 82.5% after 30 cycles are obtained; the discharge capacity is decreased as the temperature increased from 303 K to 333 K; the alloy electrode has higher discharge capacity within the discharge current density span from 60 mA g^{-1} to 300 mA g^{-1}.

(3) The charge transfer resistance R_T on the alloy surface is 0.135 Ω and the exchange current density I_0 is 1298 mA g^{-1}, respectively.

(4) The self-discharge rate of the alloy electrode is increased as the time standing increases (increased), and also the reversible part (C_3-C_2) is larger than that of irreversible (C_1–C_3) part.

Conflict of Interests

The authors declare that they have no conflict of interests.

Acknowledgments

This work was supported by Ministry of Science and Technology of China (2011AA03A408), the Foundation of State Key Laboratory of Rare Earth Resources Utilization (RERU2013021), and Doctoral Foundation of Yanshan University (B330).

References

[1] J. J. Liu, S. M. Han, Y. Li et al., "Phase structure and electrochemical characteristics of high-pressuresintered La–Mg–Ni-based hydrogen storage alloys," *Electrochimica Acta*, vol. 111, pp. 18–24, 2013.

[2] L. Zhang, S. M. Han, Y. Li et al., "Formation mechanism, phase structure and electrochemical properties of the La–Mg–Ni-based multiphase alloys by powder sintering $LaNi_5$ and $LaMgNi_4$," *International Journal of Hydrogen Energy*, vol. 38, no. 25, pp. 10431–10437, 2013.

[3] J. L. Zhang, S. M. Han, Y. Li et al., "Effects of $PuNi_3$and Ce_2Ni_7-type phase abundance on electrochemical characteristics of La–Mg–Ni-based alloys," *Journal of Alloys and Compounds*, vol. 581, pp. 693–698, 2013.

[4] C. C. Nwakwuo, T. Holm, R. V. Denys et al., "Effect of magnesium content and quenching rate on the phase structure and composition of rapidly solidified La_2MgNi_9 metal hydride battery electrode alloy," *Journal of Alloys and Compounds*, vol. 555, pp. 201–208, 2013.

[5] Y. H. Zhang, Z. H. Hou, B. W. Li, H. P. Ren, G. F. Zhang, and D. L. Zhao, "An investigation on electrochemical hydrogen storage performances of the as-cast and -annealed $La_{0.8-x}Sm_xMg_{0.2}Ni_{3.35}Al_{0.1}Si_{0.05}$(x = 0–0.4) alloys," *Journal of Alloys and Compounds*, vol. 537, pp. 175–182, 2013.

[6] B. P. Wang, Y. Z. Chen, and Y. N. Liu, "Structure and electrochemical properties of $(La_{1-x}Dy_x)_{0.8}Mg_{0.2}Ni_{3.4}Al_{0.1}$ (x = 0.0–0.20) hydrogen storage alloys," *International Journal of Hydrogen Energy*, vol. 37, no. 11, pp. 9082–9087, 2012.

[7] H. X. Huang and K. L. Huang, "Effect of AB_5 alloy on electrochemical properties of $Mm_{0.80}Mg_{0.20}Ni_{2.56}Co_{0.50}Mn_{0.14}Al_{0.12}$ hydrogen storage alloy," *Powder Technology*, vol. 221, pp. 365–370, 2012.

[8] X. P. Dong, L. Y. Yang, X. T. Li, Q. Wang, L. H. Ma, and Y. F. Lin, "Effect of substitution of aluminum for nickel on electrochemical properties of $La_{0.75}Mg_{0.25}Ni_{3.5-x}Co_{0.2}Al_x$ hydrogen storage alloys," *Journal of Rare Earths*, vol. 29, no. 2, pp. 143–149, 2011.

[9] Y. H. Zhang, Y. Cai, C. Zhao, T. T. Zhai, G. F. Zhang, and D. L. Zhao, "Electrochemical performances of the as-melt $La_{0.75-x}M_xMg_{0.25}Ni_{3.2}Co_{0.2}Al_{0.1}$(M = Pr, Zr, x = 0, 0. 2) alloys applied to Ni/metal hydride (MH) battery," *International Journal of Hydrogen Energy*, vol. 37, no. 19, pp. 14590–14597, 2012.

[10] Y. Liu, Y. Cao, L. Huang, M. Gao, and H. Pan, "Rare earth–Mg–Ni-based hydrogen storage alloys as negative electrode materials for Ni/MH batteries," *Journal of Alloys and Compounds*, vol. 509, no. 3, pp. 675–686, 2011.

[11] K. Kadir, T. Sakai, and I. Uehara, "Synthesis and structure determination of a new series of hydrogen storage alloys; RMg_2Ni_9 (R = La, Ce, Pr, Nd, Sm and Gd) built from $MgNi_2$ laves-type layers alternating with AB_5 layers," *Journal of Alloys and Compounds*, vol. 257, no. 1-2, pp. 115–121, 1997.

[12] K. Kadir, N. Kuriyama, T. Sakai, I. Uehara, and L. Eriksson, "Structural investigation and hydrogen capacity of $CaMg_2Ni_9$: a new phase in the AB_2C_9 system isostructural with $LaMg_2Ni_9$," *Journal of Alloys and Compounds*, vol. 284, no. 1-2, pp. 145–154, 1999.

[13] K. Kadir, T. Sakai, and I. Uehara, "Structural investigation and hydrogen storage capacity of $LaMg_2Ni_9$ and $(La_{0.65}Ca_{0.35})(Mg_{1.32}Ca_{0.68})Ni_9$ of the AB_2C_9 type structure," *Journal of Alloys and Compounds*, vol. 302, no. 1-2, pp. 112–117, 2000.

[14] J. Chen, H. T. Takeshita, H. Tanaka et al., "Hydriding properties of $LaNi_3$ and $CaNi_3$ and their substitutes with $PuNi_3$-type structure," *Journal of Alloys and Compounds*, vol. 302, no. 1-2, pp. 304–313, 2000.

[15] B. Liao, Y. Q. Lei, L. X. Chen, G. L. Lu, H. G. Pan, and Q. D. Wang, "The structural and electrochemical properties of $La_2Mg(Ni_{0.8-x}Co_{0.2}Al_x)_9$ (x = 0−0.03) hydrogen storage electrode alloys," *Journal of Alloys and Compounds*, vol. 415, no. 1-2, pp. 239–243, 2006.

[16] B. Liao, Y. Q. Lei, L. X. Chen, G. L. Lu, H. G. Pan, and Q. D. Wang, "Effect of the La/Mg ratio on the structure and electrochemical properties of $La_xMg_{3-x}Ni_9$ (x = 1.6–2.2) hydrogen storage electrode alloys for nickel-metal hydride batteries," *Journal of Power Sources*, vol. 129, no. 2, pp. 358–367, 2004.

[17] H. Miao, H. Pan, S. C. Zhang, N. Chen, R. Li, and M. X. Gao, "Influences of Co substitution and annealing treatment on the structure and electrochemical properties of hydrogen storage alloys $La_{0.7}Mg_{0.3}Ni_{2.45-x}Co_{0.75+x}Mn_{0.1}Al_{0.2}$ ($x = 0.00, 0.15, 0.30$)," *International Journal of Hydrogen Energy*, vol. 32, no. 15, pp. 3387–3394, 2007.

[18] H. G. Pan, Y. F. Liu, M. X. Gao, R. Li, and Y. Q. Lei, "Function of cobalt in the new type rare-earth Mg-based hydrogen storage electrode alloys," *Intermetallics*, vol. 13, no. 7, pp. 770–777, 2005.

[19] B. Liao, Y. Q. Lei, L. X. Chen, G. L. Lu, H. G. Pan, and Q. D. Wang, "Effect of Co substitution for Ni on the structural and electrochemical properties of $La_2Mg(Ni_{1-x}Co_x)_9$ (x = 0.1– 0.5) hydrogen storage electrode alloys," *Electrochimica Acta*, vol. 50, no. 4, pp. 1057–1063, 2004.

[20] B. Liao, Y. Q. Lei, L. X. Chen, G. L. Lu, H. G. Pan, and Q. D. Wang, "The effect of Al substitution for Ni on the structure and electrochemical properties of AB_3-type $La_2Mg(Ni_{1-x}Al_x)_9$ (x = 0–0.05) alloys," *Journal of Alloys and Compounds*, vol. 404–406, pp. 665–668, 2005.

[21] X.-Y. Zhang, Y.-C. Luo, D.-H. Wang, R.-X. Yan, Y. Zhang, and L. Kang, "A study on the structure and electrochemical properties of $La_{0.67}Mg_{0.33}Ni_{3.0-x}Al_x$ (x = 0, 0.1, 0.2, 0.3) hydrogen storage alloys," *Journal of Functional Materials*, vol. 36, no. 7, pp. 1034–1040, 2005.

[22] B. P. Wang, Y. Z. Chen, and Y. N. Liu, "Structure and electrochemical properties of $(La_{1-x}\ Dy_x)_{0.8}Mg_{0.2}Ni_{3.4}Al_{0.1}$ (x = 0.0–0.20) hydrogen storage alloys," *International Journal of Hydrogen Energy*, vol. 37, no. 11, pp. 9082–9087, 2012.

[23] J. B. Fan, A. Q. Deng, G. J. Xia, K. N. Qian, and Y. C. Luo, "Phase structure and electrochemical properties of the $AB_{3.8}$-type La–Mg–Ni system hydrogen storage alloys," *Rare Metal Materials and Engineering*, vol. 39, no. 12, pp. 2142–2146, 2010.

[24] Y. Q. Qiao, M. S. Zhao, X. J. Zhu, and G. Cao, "Microstructure and some dynamic performances of $Ti_{0.17}Zr_{0.08}V_{0.34}RE_{0.01}Cr_{0.1}Ni_{0.3}$(RE = Ce, Dy) hydrogen storage electrode alloys," *International Journal of Hydrogen Energy*, vol. 32, no. 15, pp. 3427–3434, 2007.

[25] H. Miao, H. Pan, S. Zhang, N. Chen, R. Li, and M. Gao, "Influences of Co substitution and annealing treatment on the structure and electrochemical properties of hydrogen storage alloys $La_{0.7}Mg_{0.3}Ni_{2.45-x}Co_{0.75+x}Mn_{0.1}Al_{0.2}$ ($x = 0.00, 0.15, 0.30$)," *International Journal of Hydrogen Energy*, vol. 32, no. 15, pp. 3387–3394, 2007.

[26] N. Kuriyama, T. Sakai, H. Miyamura, I. Uehara, H. Ishikawa, and T. Iwasaki, "Electrochemical impedance and deterioration behavior of metal hydride electrodes," *Journal of Alloys and Compounds*, vol. 202, no. 1-2, pp. 183–197, 1993.

[27] C. Iwakura, T. Askahiko, H. Yoneyama, T. Sakai, K. Oguro, and H. Ishikawa, "Electrochemical characteristics of $LaNi_5$ system hydrogen-absorbing alloys as negative electrode materials for nickel-hydrogen batteries," *The Chemical Society of Japan*, vol. 8, pp. 1482–1488, 1988.

[28] Y. Q. Qiao, M. S. Zhao, M. Y. Li, X. J. Zhu, and G. Y. Cao, "Microstructure and electrochemical performance of $Ti_{0.17}Zr_{0.08}V_{0.34}Pd_{0.01}Cr_{0.1}Ni_{0.3}$ electrode alloy," *Scripta Materialia*, vol. 55, no. 3, pp. 279–282, 2006.

[29] C. Iwakura, Y. Kajiya, H. Yoneyama, T. Saki, K. Oguro, and H. Ishikawa, "Self-discharge mechanism of nickel-hydrogen batteries using metal hydride anodes," *Journal of the Electrochemical Society*, vol. 136, no. 5, pp. 1351–1355, 1989.